Chemistry–A European Journal
Minireview
doi.org/10.1002/chem.202102224
Chemistry Europe
European Chemical Societies Publishing

Special Collection

Liquid-Crystalline Polymer Particles Prepared by Classical Polymerization Techniques

Xiaohong Liu,[a, b] Michael G. Debije,[a] Johan P. A. Heuts,*[a, b] and Albert P. H. J. Schenning*[a, b]

To commemorate prof. François Diederich and in gratitude to his mentorship

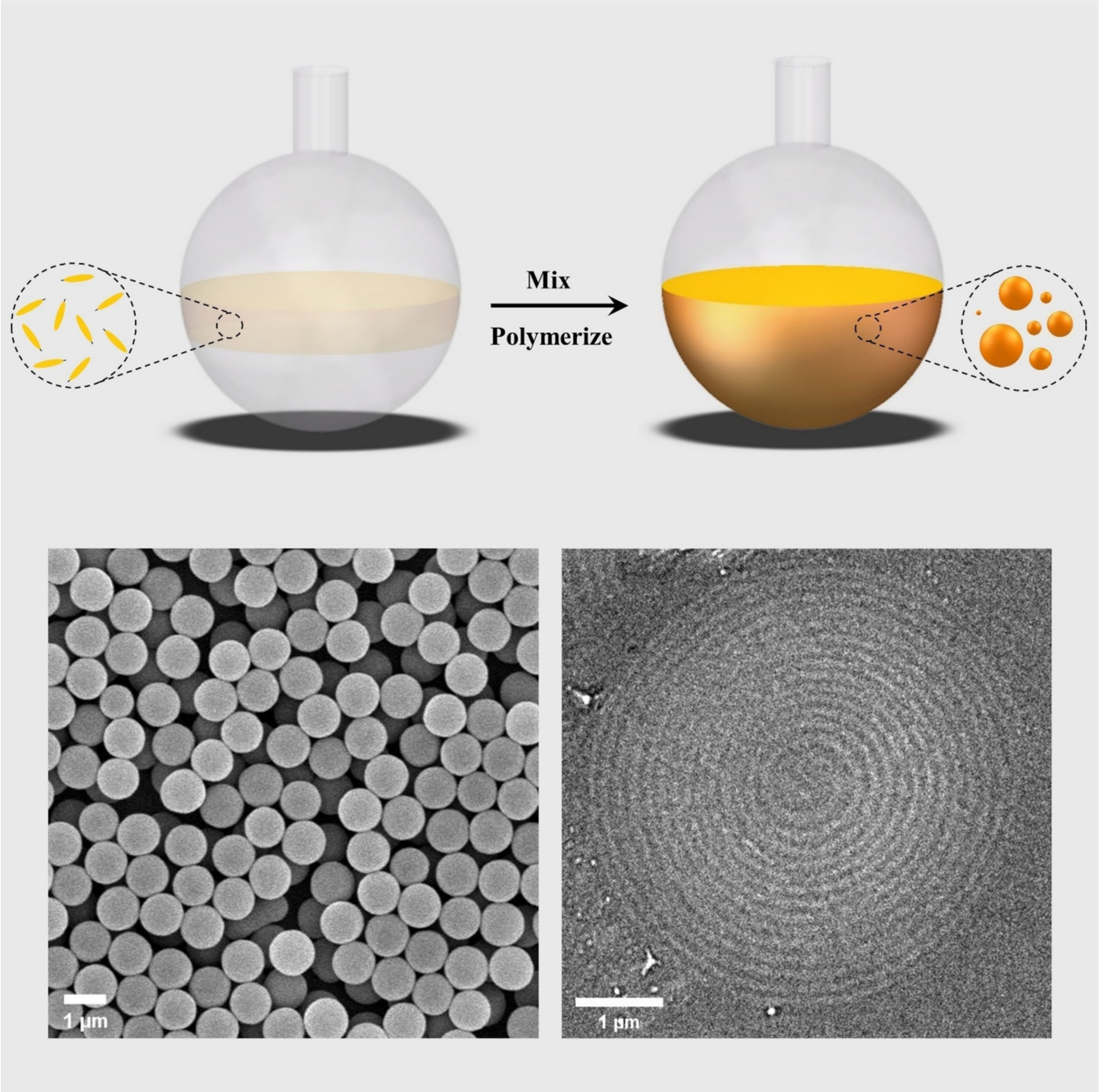

Abstract: Liquid-crystalline polymer particles prepared by classical polymerization techniques are receiving increased attention as promising candidates for use in a variety of applications including micro-actuators, structurally colored objects, and absorbents. These particles have anisotropic molecular order and liquid-crystalline phases that distinguish them from conventional polymer particles. In this minireview, the preparation of liquid-crystalline polymer particles from classical suspension, (mini-)emulsion, dispersion, and precipitation polymerization reactions are discussed. The particle sizes, molecular orientations, and liquid-crystalline phases produced by each technique are summarized and compared. We conclude with a discussion of the challenges and prospects of the preparation of liquid-crystalline polymer particles by classical polymerization techniques.

1. Introduction

Liquid crystals have unique properties which make them attractive for the preparation of polymer particles. The liquid-crystalline (LC) state is a phase between solid crystals and isotropic liquids in which molecules preserve some degree of the molecular order of a crystal but flow like a liquid. Molecules that show a LC state in a specific temperature range are called thermotropic LCs, and these molecules usually are geometrically anisotropic, often rod-like.[1,2] LC phases can be further categorized based on the organization of the individual molecules (Figure 1).[3,4] For instance, LC molecules in the nematic phase have no positional order but directional order described by the "molecular director", while LC molecules in the smectic phase have both positional and orientational order and form layers. Chiral nematic (or cholesteric) LC molecules are rotated along the axis perpendicular to the molecular director, and the distance for the molecular director to rotate over 360° is defined as the pitch.

The self-assembly of LCs can be controlled by aligning LC molecules with surface alignment layers,[5] mechanical forces,[6] or external electric fields,[7] and by doing so bulk LC materials with macroscopic anisotropy can be obtained.[8–10] When liquid-crystalline molecules are equipped with polymerizable units (Figure 1), the liquid-crystalline phase can be fixed by polymerization allowing a wide variety of polymer films, fibers and particles with different alignments and molecular organization.

LC polymer particles are a class of microscopic LC materials with a typical diameter less than 1 mm that exhibit anisotropic functionalities not found in amorphous polymer particles, and have been suggested for use as micropumps,[11] actuators,[12,13] and light reflectors.[14] A widely applied method to prepare LC polymer particles is microfluidics, as highly monodisperse, monodomain, multi-structured particles with typical dimensions between 100 μm–1 mm and a variety of morphologies can be prepared.[15–19] Nevertheless, the preparation of smaller LC polymer particles ($d < 10$ μm) through microfluidics becomes increasingly challenging when attempting to further reduce the particle size and has not been reported, probably since the narrower micro-channels might be clogged by the monomer droplets and polymerized particles during preparation.[20] On the other hand, classical polymerization techniques can be readily applied for the preparation of smaller particles. Classical polymerization techniques, including suspension, mini-emulsion, dispersion, and precipitation polymerizations, are more suitable for preparing smaller LC polymer particles (Figure 2a).[21] Suspension polymerization has been widely applied to prepare LC polymer particles with an average diameter > 1 μm. LC polymer particles with various LC phases and alignments have been successfully prepared, with both the

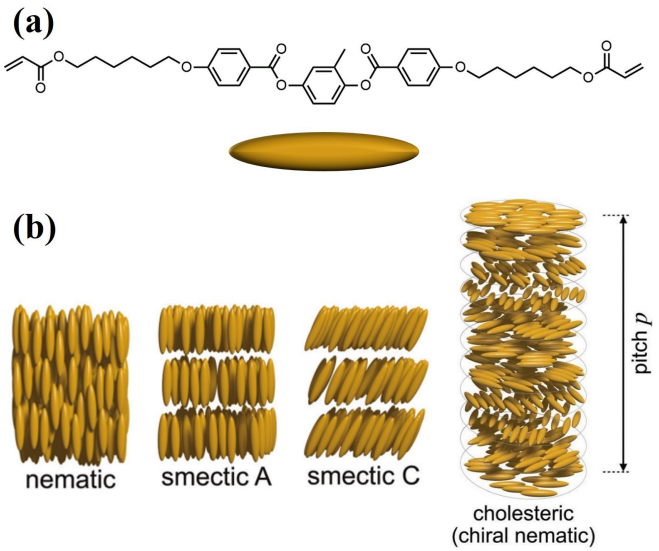

Figure 1. a) An example of the chemical structure of a rod-like LC molecule. b) Schematic representation of the molecular alignment in various LC phases. Reproduced with permission from ref. [4]. Copyright: 2016 The Royal Society of Chemistry.

[a] *X. Liu, Dr. M. G. Debije, Dr. J. P. A. Heuts, Prof. Dr. A. P. H. J. Schenning*
Department of Chemical Engineering and Chemistry
Eindhoven University of Technology
PO Box 513, 5600 MB, Eindhoven (The Netherlands)
E-mail: j.p.a.heuts@tue.nl
a.p.h.j.schenning@tue.nl
[b] *X. Liu, Dr. J. P. A. Heuts, Prof. Dr. A. P. H. J. Schenning*
Institute for Complex Molecular Systems
Eindhoven University of Technology
PO Box 513, 5600 MB, Eindhoven (The Netherlands)

Special Collection *This article belongs to a Joint Special Collection dedicated to François Diederich.*

phase and alignment having profound influences on the properties of the LC polymer particles. In mini-emulsion polymerization, the average diameter is reduced to <1 μm: due to the resolution of polarized optical microscopy (POM), the specific alignment usually remains unidentified. Dispersion and precipitation polymerizations start as homogeneous systems, with monomers dissolved in a solvent. During polymerization, propagating chains precipitate from the solvent and form preliminary particles that grow into final particles. The alignment can be controlled with the solvent/surfactant mixture in dispersion polymerization. Precipitation polymerization is less sensitive to the monomer composition, and hence more versatile, but the control on the alignment has not yet been explored. This minireview focuses on the preparation of LC polymer particles with a diameter <10 μm by these classical

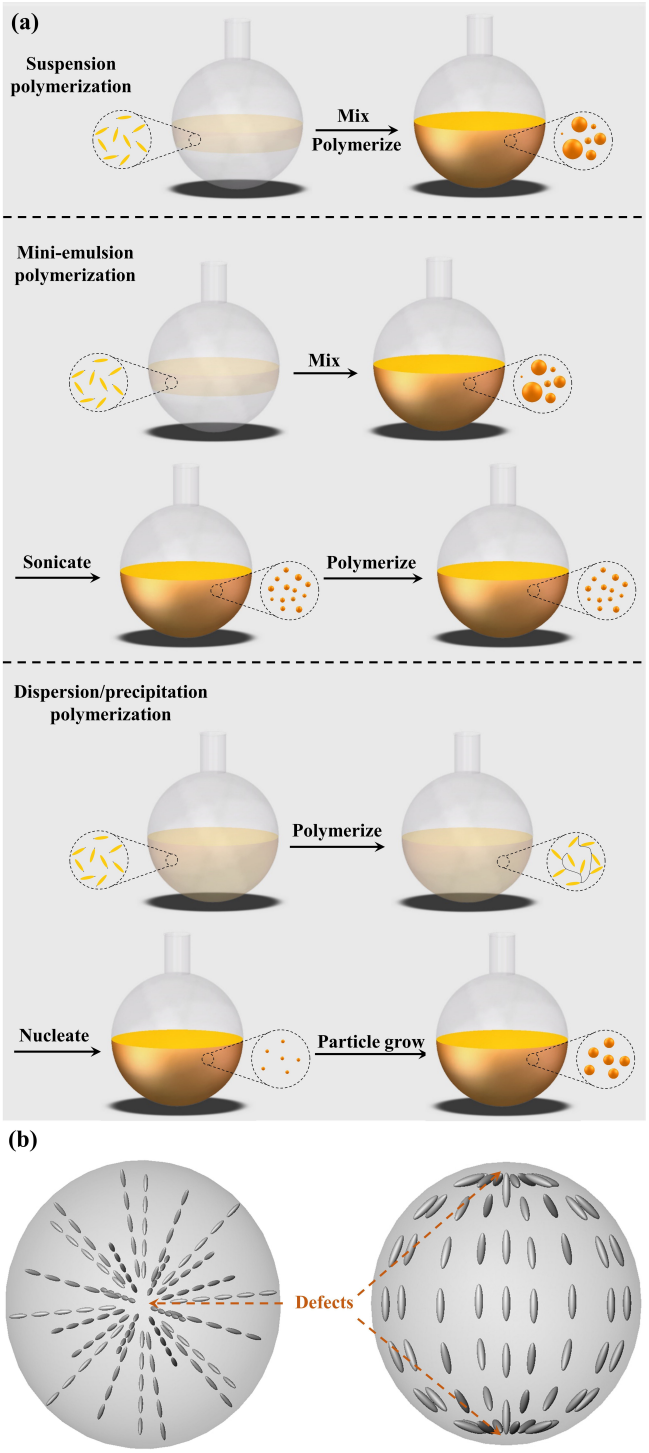

Figure 2. a) Schematic representation of classical polymerization techniques. b) Schematic representation of radial (left) and bipolar (right) alignment of liquid crystal molecules in spherical particles.

Xiaohong Liu studied material science and engineering at the South China University of Technology and graduated in 2016. After receiving a MSc in polymer science from the University of Akron, USA, he started pursuing a PhD in Stimuli-Responsive Functional Materials and Devices (SFD) group under the supervision of Prof. Albert Schenning.

Michael Debije received a MSc in high-energy physics from Iowa State University (USA) in 1994 with a thesis describing a theoretical treatment of a new breast tumor detector. In 2000, he moved to the University of Rochester (USA) where he received a PhD in Biophysics for his study of radical transport and trapping in oligonucleotide crystals of DNA. He is currently an Assistant Professor and responsible for the Energy Cluster within the Stimuli-Responsive Functional Materials and Devices (SFD) group.

Hans Heuts studied chemical engineering at Eindhoven University of Technology (TU/e) and graduated cum laude in 1992. He obtained his PhD from the University of Sydney (USyd) in 1997 under supervision of Bob Gilbert (USyd) and Leo Radom (Australian National University). In November 2005, he moved to TU/e and first joined the Polymer Chemistry research group; mid 2014 he moved to the Supramolecular Polymer Chemistry group.

Albert Schenning studied chemistry at Radboud University Nijmegen, where he obtained his master's degree in 1992 and his doctorate in 1996. He was a post-doctoral researcher at the ETH Zürich under the supervision of François Diederich. He is currently a full professor within the Stimuli-Responsive Functional Materials and Devices (SFD) group at TU/e.

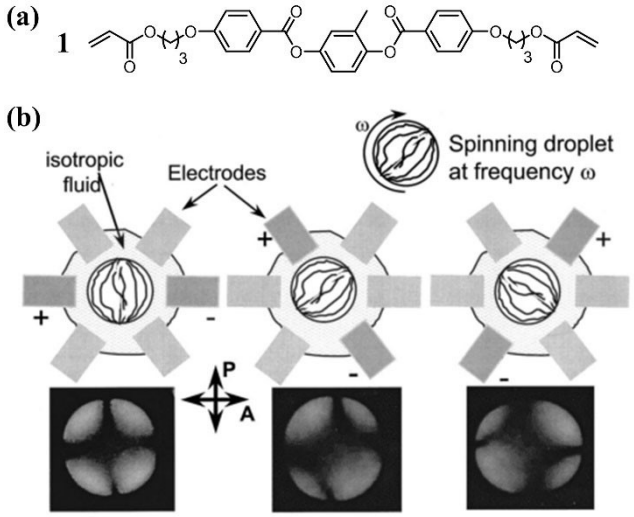

Figure 3. a) The chemical structure of RM257 (**1**). b) Schematic representation of the rotation of an LC polymer particle with an applied electric field and the corresponding change in birefringence pattern in the POM images. Reprinted with permission from ref. [23]. Copyright: 2001, AIP Publishing.

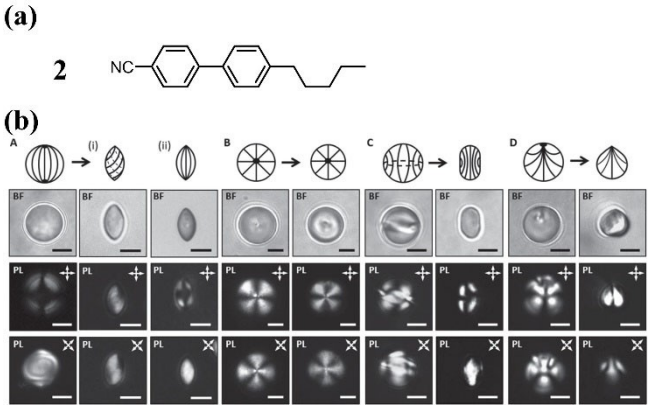

Figure 4. a) The chemical structure of 5CB (**2**). b) Schematic representation and POM images of LC polymer particle with bipolar (A), radial (B), axial (C), and preradial (D) alignment. The left and right columns are the particles before and after extraction of 5CB. Reprinted with permission from ref. [26]. Copyright: 2016, Wiley.

polymerization techniques. Previous publications on LC polymer particles with a wide range of particle sizes, chemical structures, and LC phases are summarized in Table 1 and the control of the alignment of LC molecules is discussed.

2. Suspension Polymerization

Suspension polymerization starts with adding LC monomers and initiators to an immiscible solvent, and then agitating to form a micron-size droplets suspension. The temperature is then adjusted so the molecules are in the LC phase, and the monomer droplets are then polymerized to yield the LC polymer particles. It is noteworthy that photoinitiators are commonly used to start the polymerization rather than thermal initiators so the polymerization can be conducted at any temperature and so fix the particles in different liquid crystal phases and alignments.

The first preparation of LC polymer particles by suspension photopolymerization involved an LC monomer, RM257 (Figure 3a, **1**), and a photoinitiator in glycerol at 90 °C (in the nematic phase).[22,23] Although no average diameter was reported, scanning electron microscopy (SEM) and POM images showed that at least some of the polymer particles were larger than 5 μm in diameter. The LC molecules in the monomer droplets showed a bipolar alignment (Figure 2b) which was preserved in the final LC polymer particles that was stable over a wide temperature range. This bipolar alignment resulted in a net dipole moment which interacted with an applied in-plane electric field which was used to rotate the particles (Figure 3b), this rotation monitored by changes in the birefringence pattern under POM.

LC polymer particles with internal free volume that shrank anisotropically were prepared by adding a non-polymerizable LC molecule, 5CB (Figure 4, **2**), to the same LC monomer mixture and subsequently removing it by washing with solvent after polymerization.[24] The LC monomer mixture (RM257/5CB = 20:80, w/w) was first suspended in a water/glycerol mixture (90% *v/v*) in the presence of fluorescence-labeled polystyrene (PS) particles and photopolymerized. POM images showed bipolar alignment of the LC polymer particles. By extracting 5CB with ethanol, the polymer particles shrank anisotropically, resulting in an ellipsoidal shape. The particles appeared bright when tilted with respect to the crossed polarizers, and dark

Table 1. Summary of classical polymerization techniques.

Technique	Suspension	Mini-emulsion	Dispersion	Precipitation
components	solvent (immiscible with monomers), initiator, LC monomers, stabilizer (optional)	solvent (immiscible with monomers), initiator, LC monomers, stabilizer	solvent (miscible with monomers), initiator, LC monomers, stabilizer	solvent (miscible with monomers), initiator, LC monomers
particle size/distribution	$d > 1$ μm/polydisperse	$d < 1$ μm/narrowly dispersed	$d \sim 1$ to 10 μm/monodisperse	$d \sim 1$ μm/monodisperse
alignment	bipolar, radial, non- uniform, cholesteric	onion-like layers, straight layers	bipolar, radial	radial
LC phases	nematic, smectic, cholesteric	nematic, smectic	nematic, smectic	smectic
drawbacks	broad size distribution	alignment is largely unrevealed	sensitive to monomer composition	non-radial alignment not reported

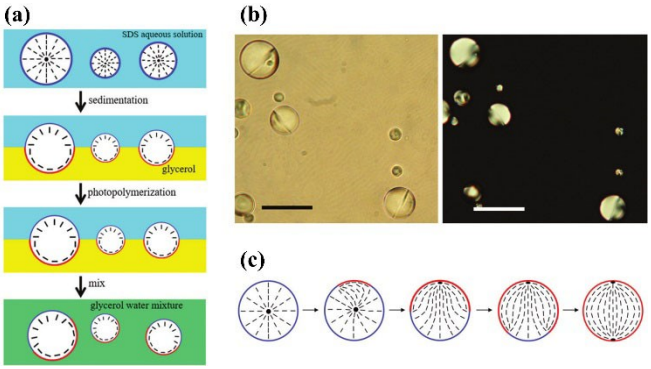

Figure 5. a) Schematic representation of the preparation of Janus LC polymer particles with coexisting radial and bipolar alignments. b) POM images of the Janus LC polymer particles without (left) and with (right) cross-polarizers. c) Schematic representation of the transformation of the LC alignment in a LC monomer droplet. Reproduced with permission from ref. [27]. Copyright: 2017, The Royal Society of Chemistry.

when parallel, indicating the bipolar alignment was maintained after the 5CB extraction, shrinkage occurring in the direction perpendicular to the line joining the two defects (Figure 2b). Fluorescence microscopy images revealed the PS particles did not randomly distribute on the surface of the LC particles, but were directed to the point defects. The direction of the PS particles was attributed to the anisotropic van der Waals interaction between PS and bipolar LC polymer particles originating from the LC alignment.[25] A further systematic investigation of RM257/5CB LC polymer particles with different cross-linking densities, alignments, and morphologies after the removal of the small molecules demonstrated that by adjusting the solvent environment and adding surfactant or colloids, the alignment of the LC polymer particles can be readily manipulated to be bipolar, radial, axial, or preradial (Figure 4b).[20,26] After the extraction of 5CB, the directional shrinkage can be programmed with the alignment, as the radial LC polymer particles showed no significant shrinkage but formed porous structures, while the LC polymer particles with other alignments shrank anisotropically, that is, perpendicular to the local director.

As the alignment in the LC polymer particles can be manipulated by the solvent,[27] RM257/5CB (**1**/**2**) monomer droplets were polymerized at the interface of an aqueous sodium dodecyl sulfate (SDS) solution and glycerol (the former induces radial and the latter bipolar alignments (Figure 5)) to create "Janus-like" LC polymer particles with non-uniform, controlled alignments. The LC monomers were first suspended in an SDS solution and aligned radially; this suspension was dropped on top of glycerol, and the monomer droplets sedimented towards the glycerol phase underneath. The mutual diffusion of water and glycerol generated a gradient in the composition of the local solvent mixture, with higher glycerol content as the LC monomer droplets sedimented. The LC

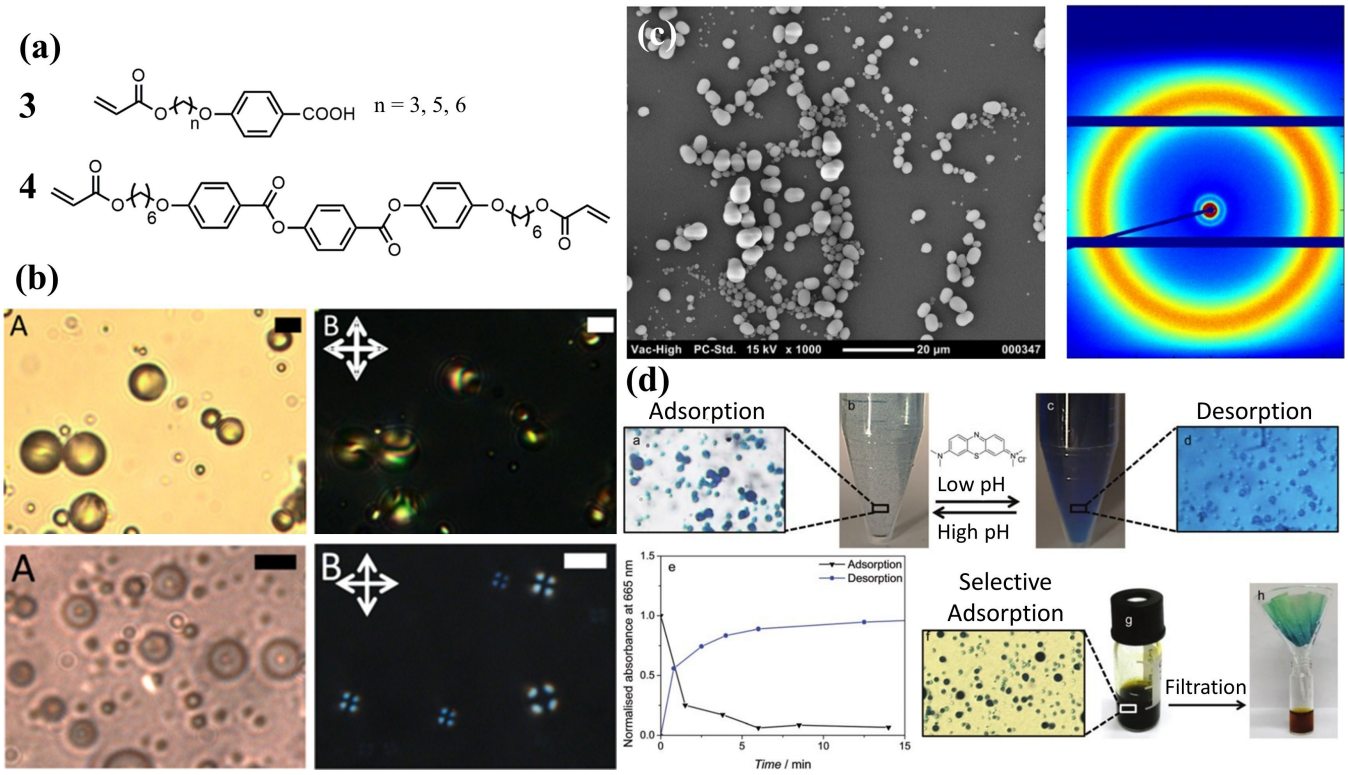

Figure 6. a) The chemical structure of the LC monomers. **3** is a mixture of three monomers in a weight ratio of 1:1:1, and a weight ratio of **3**/**4** is 9:1. b) POM images of the LC monomer droplets in nematic (top row, scale bar: 10 µm) and smectic (bottom row, scale bar: 5 µm) phases. c) SEM image (left) and XRD profile (right) of the LC polymer particles. d) Adsorption and release study of cationic/anionic dyes by the LC polymer particles. Reproduced with permission from ref. [28]. Copyright: 2016, The Royal Society of Chemistry.

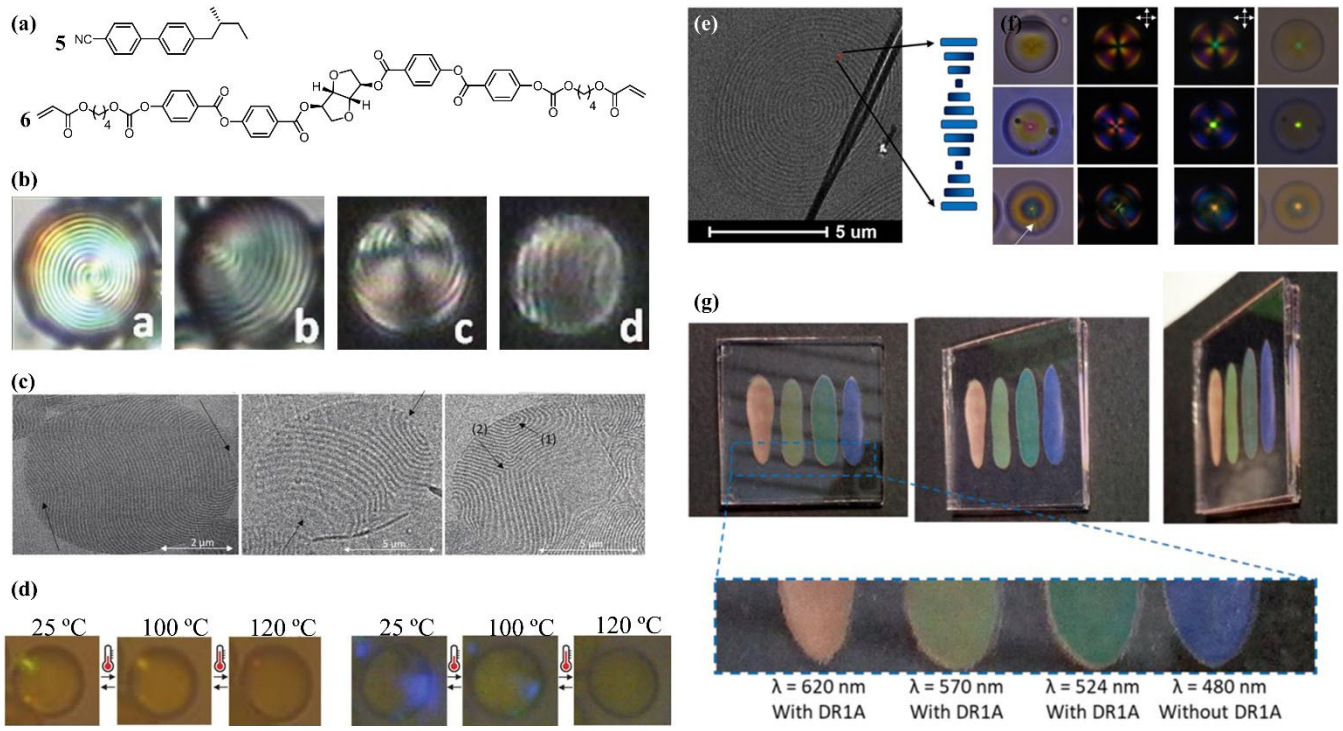

Figure 7. a) Example of a non-polymerizable (**5**) and polymerizable (**6**) chiral molecules used to induce the cholesteric phase. b) Possible LC alignments in cholesteric LC polymer particles. Images b and c are the same particles observed at different viewing angles. Reprinted with permission from ref. [39]. Copyright: 2011, Wiley. c) Transmission electron microscopy (TEM) and d) POM images of cholesteric LC polymer particles with homeotropic alignment of the LC molecules and anisotropic helical structure. Reproduced with permission from ref. [35]. Copyright: 2020, Wiley. e) TEM and f) POM images of cholesteric LC polymer particles with planar alignment of the LC molecules and concentric helical structure. g) Reflective coatings prepared with cholesteric LC polymer particles with different reflection wavelengths viewed at different angles. Reprinted with permission from ref. [34]. Copyright: 2019, The American Chemical Society.

molecules at the bottom of the droplets realigned in a bipolar alignment, while at the top the molecules retained radial alignment. Photopolymerization was performed to fix the non-uniform alignments in the LC monomer droplets and yield the Janus LC polymer particles, with both radial and bipolar alignments coexisting in the same LC polymer particles.

Suspension polymerization has also been used to prepare smectic LC polymer particles, in which LC molecules not only preserve directional order, but also form smectic layers.[28] The general procedure is similar to the preparation of nematic LC polymer particles, except that the LC monomer mixture (Figure 6a) was first suspended in the low viscosity nematic phase, and further cooled to smectic C phase for polymerization. The LC monomers showed a bipolar alignment in the nematic phase (Figure 6b top row), which rearranged into a radial alignment upon cooling to smectic C phase (Figure 6b, bottom row). Upon cooling equal quantities of enantiomeric single-domain droplets with either positive or negative tilt of the molecular orientation within the concentric layers were observed. After polymerization, the average diameter of the LC polymer particles was 1.4 μm, and the layer structure was confirmed with XRD, showing a layer spacing of 3.2 nm. Upon treating with KOH solution and deprotonating the carboxylic acid groups, the LC polymer particles showed rapid adsorption kinetics and high adsorption capacity to a cationic dye, methylene blue, while rejecting an anionic dye, methyl orange, making them promising candidates for separation and purification of chemicals.

Cholesteric LC polymer particles in which the director of LC molecules rotates periodically through the layer depth and forms a helical structure have also been prepared by suspension polymerization. The helical structure enables the cholesteric LC polymer particles to optomechanically and optically interact with light, such as generating torque and force[29–33] and reflecting light with specific wavelengths.[34–37] The monomer mixture typically consists of LC monomers with chiral molecules that induce rotation of the LC director (Figure 7a, **5** and **6**). Similar to nematic LC polymer particles, cholesteric LC polymer particles are prepared by first suspending cholesteric LC monomers in an immiscible solvent and irradiating with UV light to photopolymerize the cholesteric phase. A detailed investigation revealed that the chirality, particle size and solvent-LC interfacial properties determined the alignment of the LC molecules and their helical structure (Figure 7b),[38,39] which have a profound influence on the properties of the particles. For instance, homeotropic alignment of the LC molecules and an anisotropic helical structure led to edge-reflection (Figure 7c and d),[35] while planar alignment of the LC molecules and a concentric helical structure were found in particles with center-reflection (Figure 7e and f).[34] An interesting application of these cholesteric LC polymer particles is to

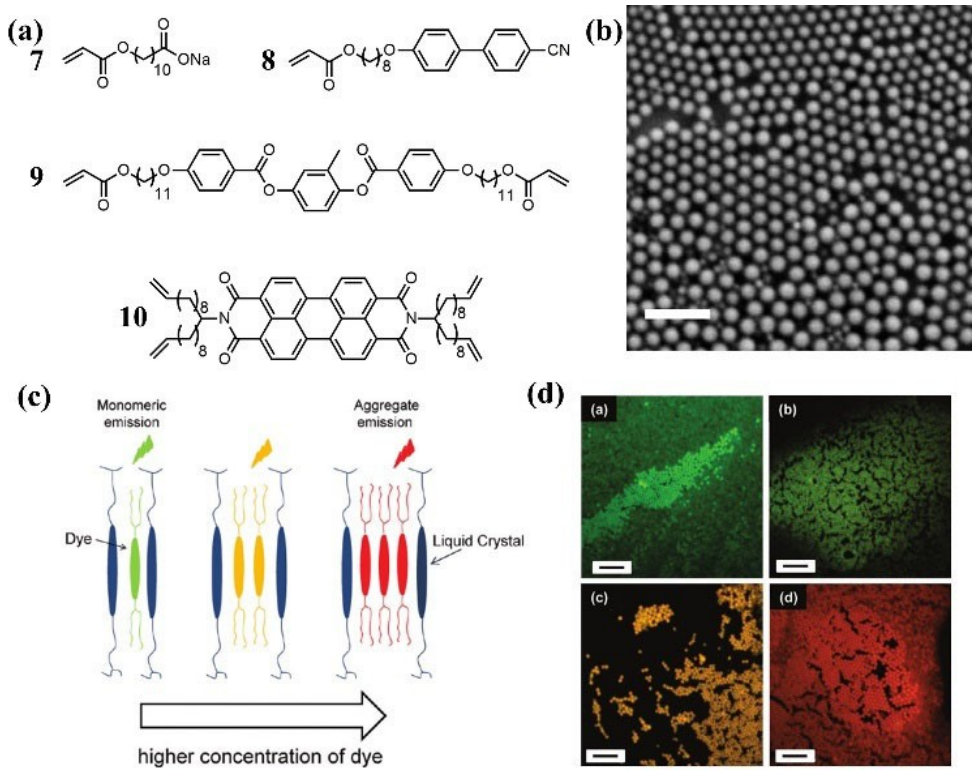

Figure 8. a) The chemical structure of AC10COONa (**7**), the LC monomers (**8** and **9**), and a fluorescence dye (**10**). b) LC polymer particles prepared with **7**, **8**, and **9**. Scale bar: 1 μm. Reprinted with permission from ref. [40]. Copyright: 2009, The American Chemical Society. c) Schematic representation of the interaction between dyes and LC molecules. d) Confocal images of fluorescent LC polymer particles with increasing dye concentration deposited on a substrate. Scale bars: 2 μm. Reprinted with permission from ref. [49]. Copyright: 2009, The American Chemical Society.

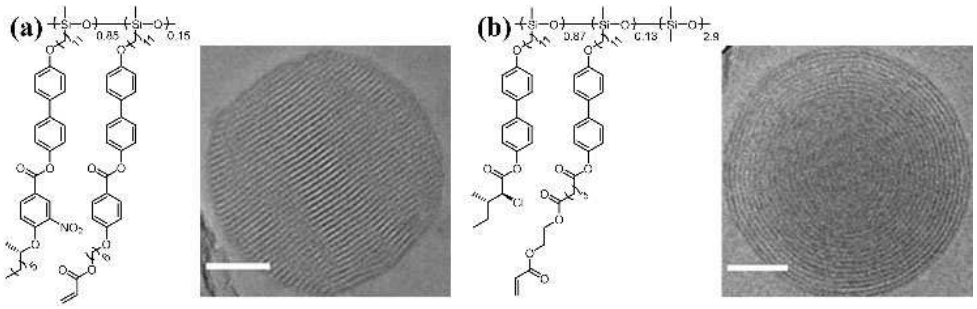

Figure 9. The chemical structure and cryo-TEM images of polysiloxane-based LC polymer particles that exhibit a) straight or b) onion-like layers. Scale bars: 50 nm. Reproduced with permission from ref. [51]. Copyright: 2005, Wiley.

produce reflective coatings by mixing the particles with a matrix with matching refractive index (Figure 7g).[34,36,37] Distinctive from cholesteric LC films, the particulate coating showed no viewing angle dependence, due to the spherical geometry of the LC polymer particles, and the color can be readily controlled with the concentration of the chiral molecules, making them an interesting and versatile multi-wavelength reflecting system.

3. Mini-emulsion Polymerization

Mini-emulsion is the only emulsion polymerization technique that has been applied to prepare LC polymer particles. Generally, the LC monomers are first added to water in the presence of a surfactant to form a suspension, followed by sonication or strong stirring to form submicron droplets before polymerization. The average diameter of the LC polymer particles prepared by mini-emulsion polymerization is generally < 1 μm.

A polymerizable surfactant, AC10COONa (**7**, Figure 8a), which consists of an acrylate and a sodium carboxylate group,

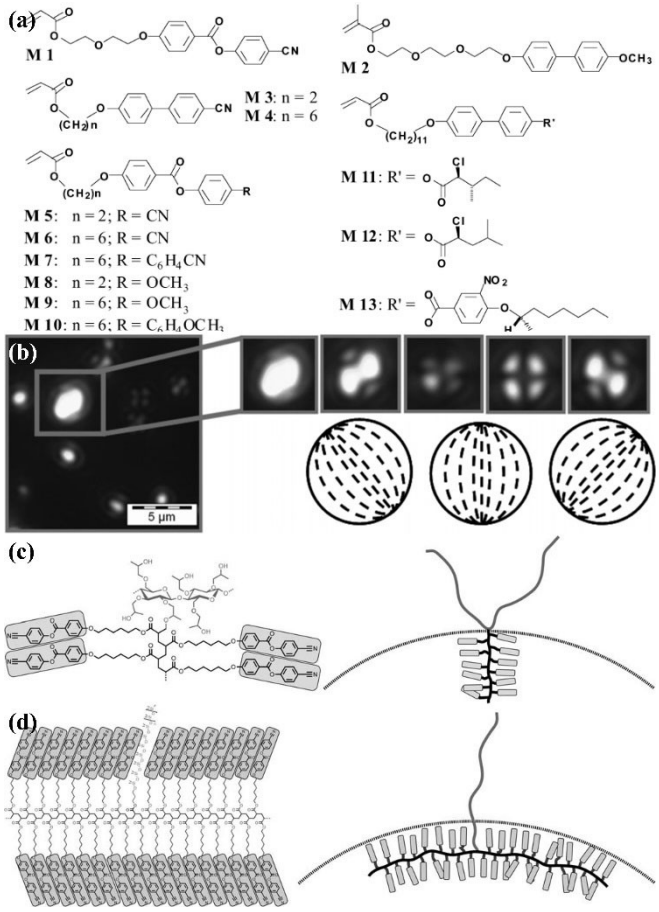

Figure 10. a) The chemical structures of the LC monomers used to prepare LC polymer particles by dispersion polymerization. b) POM images of LC polymer particles prepared from M6. The cross-polarizers were rotated to record the images in the inset. Reprinted with permission from ref. [53]. Copyright: 2006, The American Chemical Society. The proposed mechanism of the formation of the c) bipolar and d) radial LC polymer particles. Reproduced with permission from ref. [54]. Copyright: 2010, The Royal Society of Chemistry.

was used for the emulsion polymerization of LC monomers.[40] The LC monomer mixtures were first dissolved (**8** and **9**, Figure 8a) in chloroform and then added to an aqueous solution of AC10COONa and ultrasonicated to produce the mini-emulsion. The emulsion was then heated to evaporate the chloroform and polymerize the monomers, yielding LC polymer particles with an average diameter of approximately 210 nm. The electrostatic stabilization of the surfactant was critical in preventing coalescence upon drying, while steric stabilizers such as polyvinyl alcohol failed to provide stabilization, and the particles aggregated. With this surfactant, tuning both the stiffness and morphology of the LC polymer particles have been explored,[41] and the LC polymer particles have been suggested as drug delivery materials,[42–47] hosts for adjustable fluorescent dyes,[48,49] and photo-actuators.[50] For instance, fluorescent LC polymer particles were prepared with LC monomer **9** and a fluorescent dye **10**, of which the fluorescent emission redshifts upon aggregation into dimers, trimers, etc. (Figure 8c).[49] The LC molecules prevented the aggregation of the fluorescent dye and as a result enabled the tuning of the emission spectrum by the concentration of the dye (Figure 8d).

The main drawback of the mini-emulsion technique is that it is usually difficult to use POM to determine the LC alignment in the particles as the typical average diameter of the LC polymer particles prepared by mini-emulsion polymerization is $< 1\ \mu m$. In the only publication in which the LC alignment of such small LC polymer particles was successfully determined, TEM showed well-defined smectic layers in smectic polysiloxane-based LC polymer particles with an average diameter of 100–250 nm (Figure 9c and d).[51] The onion-like and straight layers were attributed to the contrast in electron density and phase separation of the polysiloxane backbone and the LC side groups. However, strict structure-alignment relationships could not be drawn.

4. Dispersion and Precipitation Polymerization

Distinct from suspension and emulsion polymerizations in which the reaction mixture is heterogeneous from the outset, dispersion polymerization starts as a homogeneous system. LC monomers, initiator, and stabilizer are first dissolved in a solvent, which is a poor or non-solvent for the polymer. With increasing molecular weight of the polymers, the solubility decreases and the polymers precipitate to form primary particles, which further grow in size to yield the final particles. The diameter is typically between sub-micron to a few microns, and narrow size distributions can be achieved with careful design of the system.

The preparation of LC polymer particles by dispersion polymerization with hydroxypropyl cellulose (HPC) as stabilizer, benzoyl peroxide (BPO) as initiator, and a mixture of ethanol and 2-methoxyethanol as solvent was explored.[52] The LC monomer (Figure 10a) and HPC were first added to the solvent and heated to the polymerization temperature (65–73 °C) for 30 min to ensure complete dissolution. BPO was added to initiate the polymerization which was carried out for 24 h to yield the LC polymer particles. The concentrations of both HPC and BPO were varied but neither showed influence on the particle size, while the solvent mixture showed a large influence. POM images reveal a "uniform director orientation" of the LC polymer particles, although the direction is not stated. A subsequent, systematic investigation in which LC polymer particles were prepared from various LC monomers and solvent mixtures by dispersion polymerization demonstrated that the dispersion polymerization method was universally applicable in preparing micron-sized LC polymer particles with a narrow size distribution from LC monomers (Figure 10a).[53] It is noteworthy that the solvent mixture needed to be carefully selected since generally larger diameters and more polydisperse particle size distributions were obtained with increasing fraction of 2-methoxyethanol, which is a good solvent for the LC monomers and polymers. Most particles showed bipolar alignment, enabling the LC polymer particles to be trapped with optical tweezers and rotated with circularly polarized light. The LC alignment

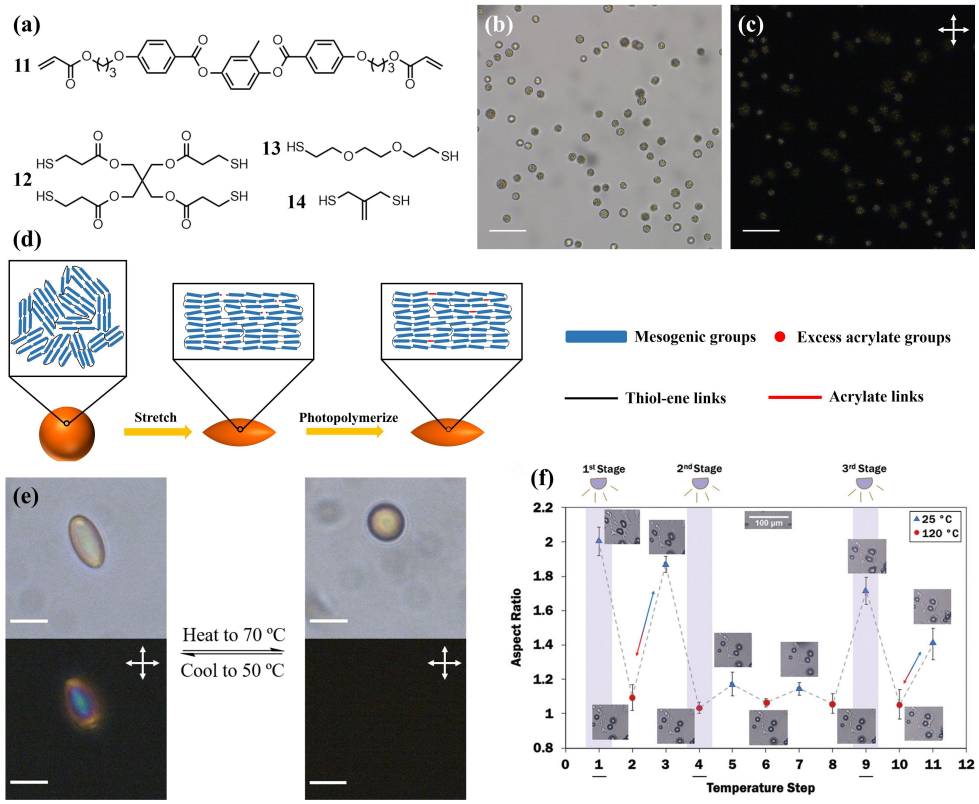

Figure 11. a) The chemical structure of the monomers used for thiol-ene dispersion polymerization. POM images of the LC polymer particles prepared from thiol-ene dispersion polymerization b) without and c) with cross-polarizers. Scale bars: 50 μm. d) Schematic representation of deforming and photo-polymerization. e) Thermal actuation of the LC polymer particles. Reproduced with permission from ref. [55]. Copyright: 2020, The Royal Society of Chemistry. f) Thermal actuation and programming of the LC polymer particles with light. Reproduced with permission from ref. [56]. Copyright: 2021, The Royal Society of Chemistry.

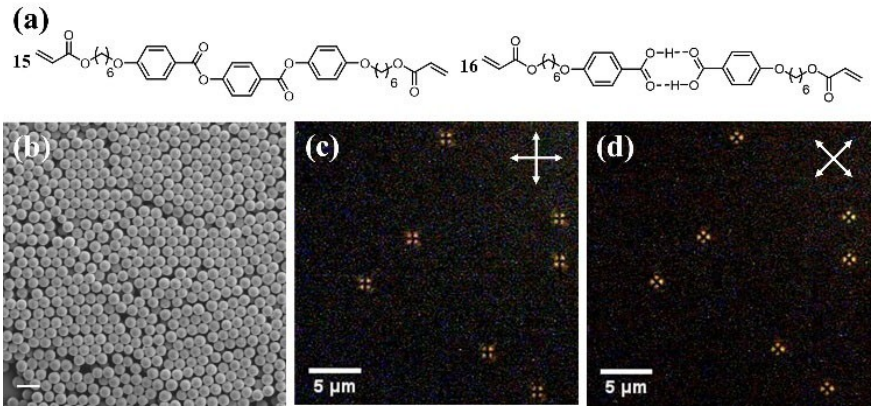

Figure 12. a) The chemical structure of the LC monomers. b) SEM (scale bar: 2 μm) and c) and d) POM images of the LC polymer particles prepared by precipitation polymerization. Adapted with permission from ref. [61]. Copyright: 2019, American Chemical Society.

can be further controlled from planar (bipolar) to homeotropic (axial or radial) by selecting the solvent/surfactant mixture.[54]

In addition to radical dispersion polymerization, thiol-ene dispersion polymerization has been applied to prepare LC polymer particles with a thiol-ene network. The monomers (Figure 11a, **11**, **12**, and **13**) and polyvinylpyrrolidone as stabilizer were first dissolved in a solvent mixture of ethanol and 2-methoxyethanol before the addition of triethylamine as catalyst.[55] The mixture was agitated overnight to yield the particles, which were 10 μm in diameter and polydomain (Figure 11b and c). The molar ratio between acrylate groups and thiol groups was 1.1, meaning residual acrylate groups are present in the LC polymer particles. A photo-initiator was introduced to the LC polymer particles, which were then

embedded in a PVA matrix. The matrix and the incorporated particles could then be deformed by stretching or compressing the matrix, followed by irradiation with UV light to photopolymerize the residual acrylate groups, forming an acrylate network independent from the existing thiol-ene network (Figure 11d). By changing the temperature of the environment, the LC phase of the LC polymer particles can be altered between the nematic and isotropic phases, and as a result, the LC polymer particles can be tuned between spherical and deformed shapes (Figure 11e). Another publication further incorporated an allyl dithiol (**14**) in the monomer mixture, which can undergo a light-initiated addition-fragmentation chain-transfer reaction, the deformed shape of such LC polymer particles can be adjusted (Figure 11f).[56]

Precipitation polymerization shares a somewhat similar mechanism and procedure with dispersion polymerization, as the system is also homogeneous at the beginning and nucleation takes place during polymerization. However, precipitation polymerization is less sensitive to specific functional groups (e.g., carboxylic acids) or cross-linkers, offering a more versatile approach.[57–60] LC polymer particles have been successfully prepared by precipitation polymerization of an LC monomer mixture consisting of benzoic-acid functionalized acrylates and LC diacrylates (Figure 12a).[61] The particle diameters were between 0.6 and 1.4 μm, mainly affected by the solvent and polymerization temperature. The polydispersity is lower than the similar particles preapred by suspension polymerization (Figure 6).[28] However, the control of alignment and preparation of non-radial LC polymer particles by precipitation polymerization have not yet been reported.[61]

5. Conclusion and Outlook

In this minireview, the preparation of LC polymer particles by classical polymerization techniques including suspension, mini-emulsion, dispersion, and precipitation polymerizations are summarized. These techniques produce LC polymer particles with various sizes, LC phases, and molecular alignments, and hence should be used in accordance with the targeted properties. Suspension polymerization has been applied to prepare LC polymer particles that are >1 μm in diameter, and the control of the alignment has also been extensively studied. More intriguingly, photonic cholesteric LC polymer particles can also be prepared by suspension polymerization. However, the size distribution of the LC polymer particles is relatively broad. LC polymer particles less than 1 μm in diameter can be prepared by mini-emulsion polymerization, but due to the small particle sizes, the internal alignment is difficult to see. Dispersion polymerization makes use of the spontaneous nucleation of the polymer chains, resulting in a very narrow particle size distribution of between 1 to 10 microns; the LC alignment can be controlled by the solvent/surfactant mixture. Precipitation polymerization is somewhat similar to dispersion polymerization but offers greater versatility, as it is less sensitive to the monomer composition, but only radial alignment has been achieved so far. These LC polymer particles have found applications as light-[33] or electricity-driven rotors,[62] absorbents,[28] cell scaffolds,[63,64] reflectors,[34] actuators,[35] and drug carriers.[47]

In general, classical polymerization techniques enable simple preparation of LC polymer particles with a diameter <10 μm, but improvements are needed before adoption by industry. For instance, although a photoinitiator is used in most suspension and emulsion polymerizations, as it can initiate over a wide temperature range, the penetration depth of the UV light is severely reduced by the high degree of scattering of the heterogeneous system, thus restricting the photopolymerization efficiency. Hence, alternative novel initiation methods that are also independent of the temperature are desired: one possibility might be redox initiators.[65] Although LC polymer particles are usually "homogeneous" in terms of chemical and physical structure, LC polymer particles with distinctive chemical domains or complex physical structures, like Janus particles, core-shell, or hollow particles, could bring more functionality and be promising directions for biomedicine, responsive microcarriers, or micro-swimmers, for example.

Acknowledgements

The authors would like to acknowledge the many discussions with and contributions of all our former and current colleagues. We are grateful for the financial support by The Netherlands Organization for scientific Research (TOP-PUNT 718.016.003).

Conflict of Interest

The authors declare no conflict of interest.

Keywords: dispersion polymerization · liquid crystal polymer particles · mini-emulsion polymerization · precipitation polymerization · suspension polymerization

[1] P. Zugenmaier, *Int. J. Mol. Sci.* **2011**, *12*, 7360–7400.
[2] M. Funahashi, T. Kato, *Liq. Cryst.* **2015**, *42*, 909–917.
[3] T. Kato, Y. Hirai, S. Nakaso, M. Moriyama, *Chem. Soc. Rev.* **2007**, *36*, 1857–1867.
[4] A. G. Dumanli, T. Savin, *Chem. Soc. Rev.* **2016**, *45*, 6698–6724.
[5] A. J. J. Kragt, D. C. Hoekstra, S. Stallinga, D. J. Broer, A. P. H. J. Schenning, *Adv. Mater.* **2019**, *31*, 1–7.
[6] P. Zhang, G. Zhou, L. T. de Haan, A. P. H. J. Schenning, *Adv. Funct. Mater.* **2021**, *31*, 1–9.
[7] H. Shimura, M. Yoshio, A. Hamasaki, T. Mukai, H. Ohno, T. Kato, *Adv. Mater.* **2009**, *21*, 1591–1594.
[8] D. Mistry, H. F. Gleeson, *J. Polym. Sci. Part B* **2019**, *57*, 1367–1377.
[9] T. Liang, H. P. C. Van Kuringen, D. J. Mulder, S. Tan, Y. Wu, Z. Borneman, K. Nijmeijer, A. P. H. J. Schenning, *ACS Appl. Mater. Interfaces* **2017**, *9*, 35218–35225.
[10] N. Herzer, H. Guneysu, D. J. D. Davies, D. Yildirim, A. R. Vaccaro, D. J. Broer, C. W. M. Bastiaansen, A. P. H. J. Schenning, *J. Am. Chem. Soc.* **2012**, *134*, 7608–7611.
[11] E. K. Fleischmann, H. L. Liang, N. Kapernaum, F. Giesselmann, J. Lagerwall, R. Zentel, *Nat. Commun.* **2012**, *3*, 1178.
[12] J. E. Marshall, S. Gallagher, E. M. Terentjev, S. K. Smoukov, *J. Am. Chem. Soc.* **2014**, *136*, 474–479.
[13] C. Ohm, E. K. Fleischmann, I. Kraus, C. Serra, R. Zentel, *Adv. Funct. Mater.* **2010**, *20*, 4314–4322.

[14] S. S. Lee, H. J. Seo, Y. H. Kim, S. H. Kim, *Adv. Mater.* **2017**, *29*, 1–8.
[15] C. Ohm, C. Serra, R. Zentel, *Adv. Mater.* **2009**, *21*, 4859–4862.
[16] H.-Q. Q. Chen, X.-Y. Y. Wang, H. K. Bisoyi, L.-J. J. Chen, Q. Li, *Langmuir* **2021**, *37*, 3789–3807.
[17] T. Hessberger, L. B. Braun, F. Henrich, C. Müller, F. Gießelmann, C. Serra, R. Zentel, *J. Mater. Chem. C* **2016**, *4*, 8778–8786.
[18] V. S. R. Jampani, D. J. Mulder, K. R. De Sousa, A. H. Gélébart, J. P. F. Lagerwall, A. P. H. J. Schenning, *Adv. Funct. Mater.* **2018**, *28*, 1801209.
[19] C. Ohm, N. Kapernaum, D. Nonnenmacher, F. Giesselmann, C. Serra, R. Zentel, *J. Am. Chem. Soc.* **2011**, *133*, 5305–5311.
[20] X. Wang, E. Bukusoglu, N. L. Abbott, *Chem. Mater.* **2017**, *29*, 53–61.
[21] R. Arshady, *Colloid Polym. Sci.* **1992**, *270*, 717–732.
[22] D. R. Cairns, N. S. Eichenlaub, G. P. Crawford, *Mol. Cryst. Liq. Cryst. Sci. Technol. Sect. A* **2001**, *352*, 275–282.
[23] D. R. Cairns, M. Sibulkin, G. P. Crawford, *Appl. Phys. Lett.* **2001**, *78*, 2643–2645.
[24] F. Mondiot, X. Wang, J. J. De Pablo, N. L. Abbott, *J. Am. Chem. Soc.* **2013**, *135*, 9972–9975.
[25] H. A. Fuster, X. Wang, X. Wang, E. Bukusoglu, S. E. Spagnolie, N. L. Abbott, *Sci. Adv.* **2020**, *6*, eabb1327.
[26] X. Wang, E. Bukusoglu, D. S. Miller, M. A. Bedolla Pantoja, J. Xiang, O. D. Lavrentovich, N. L. Abbott, *Adv. Funct. Mater.* **2016**, *26*, 7343–7351.
[27] X. Wang, Y. Zhou, Y. K. Kim, D. S. Miller, R. Zhang, J. A. Martinez-Gonzalez, E. Bukusoglu, B. Zhang, T. M. Brown, J. J. De Pablo, N. L. Abbott, *Soft Matter* **2017**, *13*, 5714–5723.
[28] H. P. C. Van Kuringen, D. J. Mulder, E. Beltran, D. J. Broer, A. P. H. J. Schenning, *Polym. Chem.* **2016**, *7*, 4712–4716.
[29] O. Brzobohatý, R. J. Hernández, S. Simpson, A. Mazzulla, G. Cipparrone, P. Zemánek, *Opt. Express* **2016**, *24*, 26382.
[30] R. J. Hernández, A. Mazzulla, A. Pane, K. Volke-Sepúlveda, G. Cipparrone, *Lab Chip* **2013**, *13*, 459–467.
[31] A. Mazzulla, G. Cipparrone, R. J. Hernandez, A. Pane, R. Bartolino, *Mol. Cryst. Liq. Cryst.* **2013**, *576*, 15–22.
[32] M. G. Donato, A. Mazzulla, P. Pagliusi, A. Magazzù, R. J. Hernandez, C. Provenzano, P. G. Gucciardi, O. M. Maragò, G. Cipparrone, *Sci. Rep.* **2016**, *6*, 1–7.
[33] M. G. Donato, J. Hernandez, A. Mazzulla, C. Provenzano, R. Saija, R. Sayed, S. Vasi, A. Magazzù, P. Pagliusi, R. Bartolino, P. G. Gucciardi, O. M. Maragò, G. Cipparrone, *Nat. Commun.* **2014**, *5*, 1–7.
[34] A. Belmonte, T. Bus, D. J. Broer, A. P. H. J. Schenning, *ACS Appl. Mater. Interfaces* **2019**, *11*, 14376–14382.
[35] A. Belmonte, Y. Y. Ussembayev, T. Bus, I. Nys, K. Neyts, A. P. H. J. Schenning, *Small* **2020**, *16*, 1905219.
[36] A. Belmonte, M. Pilz da Cunha, K. Nickmans, A. P. H. J. Schenning, *Adv. Opt. Mater.* **2020**, *8*, 2000054.
[37] E. Beltran-Gracia, O. L. Parri, *J. Mater. Chem. C* **2015**, *3*, 11335–11340.
[38] C. Provenzano, A. Mazzulla, P. Pagliusi, M. P. De Santo, G. Desiderio, I. Perrotta, G. Cipparrone, *APL Mater.* **2014**, *2*, 0–7.
[39] G. Cipparrone, A. Mazzulla, A. Pane, R. J. Hernandez, R. Bartolino, *Adv. Mater.* **2011**, *23*, 5773–5778.
[40] C. M. Spillmann, J. Naciri, K. J. Wahl, Y. H. Garner, M. S. Chen, B. R. Ratna, *Langmuir* **2009**, *25*, 2419–2426.
[41] J. C. Zhou, S. Tsoi, C. M. Spillmann, J. Naciri, B. Ratna, *J. Colloid Interface Sci.* **2012**, *368*, 152–157.
[42] O. K. Nag, J. Naciri, E. Oh, C. M. Spillmann, J. B. Delehanty, *Bioconjugate Chem.* **2016**, *27*, 982–993.
[43] O. K. Nag, J. Naciri, J. S. Erickson, E. Oh, J. B. Delehanty, *Bioconjugate Chem.* **2018**, *29*, 2701–2714.
[44] O. K. Nag, J. B. Delehanty, J. Naciri, *Colloid. Nanoparticles Biomed. Appl. XIII* **2018**, 1050711.
[45] O. K. Nag, J. Naciri, E. Oh, C. M. Spillmann, J. B. Delehanty, *J. Visualization* **2017**, *2017*, 1–8.
[46] O. K. Nag, J. Naciri, C. M. Spillmann, J. B. Delehanty, *Colloid. Nanoparticles Biomed. Appl. XI* **2016**, 972215.
[47] C. M. Spillmann, J. Naciri, W. R. Algar, I. L. Medintz, J. B. Delehanty, *ACS Nano* **2014**, *8*, 6986–6997.
[48] J. Li, M. Tian, H. Xu, X. Ding, J. Guo, *Part. Part. Syst. Charact.* **2019**, *36*, 1–8.
[49] C. M. Spillmann, J. Naciri, G. P. Anderson, M. S. Chen, B. R. Ratna, *ACS Nano* **2009**, *3*, 3214–3220.
[50] S. Tsoi, J. Zhou, C. Spillmann, J. Naciri, T. Ikeda, B. Ratna, *Macromol. Chem. Phys.* **2013**, *214*, 734–741.
[51] M. Vennes, R. Zentel, M. Rössle, M. Stepputat, U. Kolb, *Adv. Mater.* **2005**, *17*, 2123–2127.
[52] M. Vennes, R. Zentel, *Macromol. Chem. Phys.* **2004**, *205*, 2303–2311.
[53] M. Vennes, S. Martin, T. Gisler, R. Zentel, *Macromolecules* **2006**, *39*, 8326–8333.
[54] S. Haseloh, P. Van Der Schoot, R. Zentel, *Soft Matter* **2010**, *6*, 4112–4119.
[55] X. Liu, X. Pan, M. G. Debije, J. P. A. Heuts, D. J. Mulder, A. P. H. J. Schenning, *Soft Matter* **2020**, *16*, 4908–4911.
[56] A. M. Martinez, L. M. Cox, J. P. Killgore, N. J. Bongiardina, R. D. Riley, C. N. Bowman, *Soft Matter* **2021**, *17*, 467–474.
[57] T. Nakano, N. Saito, H. Minami, *Langmuir* **2020**, *36*, 11957–11962.
[58] J. S. Song, L. Chagal, M. A. Winnik, *Macromolecules* **2006**, *39*, 5729–5737.
[59] J. S. Song, M. A. Winnik, *Macromolecules* **2005**, *38*, 8300–8307.
[60] K. Li, H. D. H. Stöver, *J. Polym. Sci. Part A* **1993**, *31*, 3257–3263.
[61] X. Liu, Y. Xu, J. P. A. Heuts, M. G. Debije, A. P. H. J. Schenning, *Macromolecules* **2019**, *52*, 8339–8345.
[62] S. Haseloh, R. Zentel, *Macromol. Chem. Phys.* **2009**, *210*, 1394–1401.
[63] T. Bera, C. Malcuit, R. J. Clements, E. Hegmann, *Front. Mater.* **2016**, *3*, 1–8.
[64] T. Bera, E. J. Freeman, J. A. McDonough, R. J. Clements, A. Aladlaan, D. W. Miller, C. Malcuit, T. Hegmann, E. Hegmann, *ACS Appl. Mater. Interfaces* **2015**, *7*, 14528–14535.
[65] N. Kohut-Svelko, R. Pirri, J. M. Asua, J. R. Leiza, *J. Polym. Sci. Part A* **2009**, *47*, 2917–2927.

Manuscript received: June 21, 2021
Accepted manuscript online: July 28, 2021
Version of record online: September 2, 2021

